near the GP may cause overgrowth of the bones [2]. Limb length discrepancy (LLD) caused by the above conditions is currently corrected by surgery if the final difference is predicted to be more than 2 cm [7]. Limb lengthening by distraction osteogenesis [9, 23, 24] is yet another option of surgical treatment.

The GP is an avascular tissue that comprises resting, proliferating and hypertrophic chondrocytes in columnar arrangement. Various cytokines and growth factors are known to affect the growth and differentiation of chondrocytes. Of these, insulin-like growth factor-I (IGF-I) is the most prominent growth factor, mediating growth hormone (GH) effects either by endocrine [3] or by autocrine/paracrine mechanisms [13]. The lack of GH or IGF-I may cause a short stature [21], while their overproduction may cause giantism or acromegaly.

Subcutaneous or intravenous administration of GH or IGF-I enhances systemic bone growth [8, 22], and recombinant human GH and IGF-I are now available to treat the GH/IGF-I-deficient patients. To date, however, no standard method has been established for controlling the growth of a particular bone by such a humeral growth factor. The patient with LLD has no choice other than undergoing surgical lengthening of the short bone, which usually requires the long-term application of a bulky external fixation device. We report here a technique for enhancing local bone growth at a selected GP by the continuous infusion of IGF-I into the epiphysis. This method does not require major surgery and is applicable for treating patients with LLD.

## Materials and methods

### Animals

Thirty-three male Japanese white rabbits (age: 4 weeks; weight: 650–800 g) were purchased from Oriental Yeast Co. (Tokyo, Japan). The animals were housed under standardised environmental conditions and fed standard rabbit chow (RC4, Oriental Yeast Co.). The control group consisted of five rabbits whose body weight and bone growth were observed but which were not operated on (intact tibia). The remaining 28 rabbits were anaesthetized with an intravenous injection of ketamine hydrochloride and xylazine at doses of 20 mg/kg and 5 mg/kg body weight, respectively. A small hole (diameter: 0.35 mm) was then drilled into the epiphysis of both proximal tibia. An L-

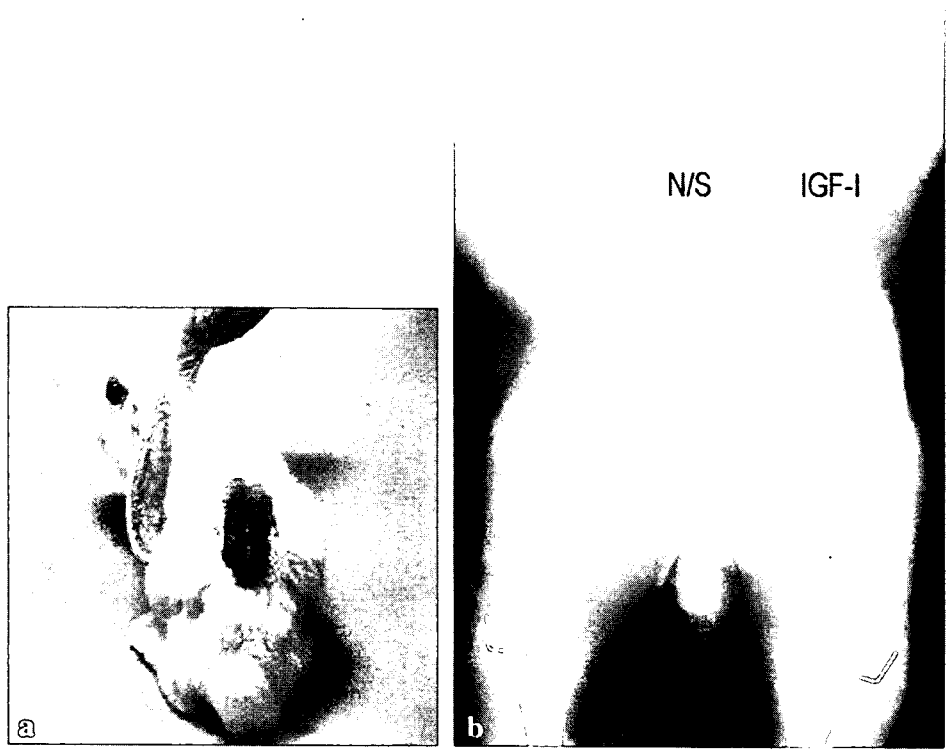


**Fig. 1** **a** A young male rabbit bearing two osmotic pumps on his back, **b** a radiograph of the animal. Each osmotic pump was connected to a radiolucent plastic catheter and aluminium canula inserted into the proximal epiphysis of the tibia. The right pump was filled with normal saline (*N/S*) and the left pump with insulin-like growth factor-I (*IGF-I*)


**Fig. 2** A radiograph of rabbit tibiae treated for 4 weeks with normal saline (*N/S*) and insulin-like growth factor-I (*IGF-I*). The IGF-I-treated tibia was 2 mm longer than the N/S-treated tibia. Note that the fibula did not show overgrowth

shaped cannula of a 28-gauge needle was inserted through the hole, and the surrounding tissues were sutured to stabilize the needle. Two ALZET osmotic pumps were implanted subcutaneously on the back of the rabbit (Fig. 1a). The left tibia was infused with IGF-I at 150 μg/kg per day through a polyethylene catheter connected to the cannula, and the right tibia was infused with normal saline (N/S) (Fig. 1b). The recombinant human IGF-I was a generous gift of Fujisawa Chemical Co. (Osaka, Japan).

The rabbits were divided into three groups based on the length of time infused with the IGF-I and N/S solutions: 1-week treatment group ($n$=5), 2-week treatment group ($n$=5) and 4-week treatment group ($n$=14). Following the treatment period, the animals were killed by sodium pentobarbitone injection (60 mg/kg body weight), and the tibiae were harvested to measure the bone mineral density (BMD) and to carry out radiological and histological analyses. This protocol was approved of by the local animal protection agency and the Ethics Committee of the University of Tokushima.

In a subset of this experiment, we performed a continuous local infusion of Indian ink at 2.5 μl/h into the proximal epiphysis of the tibia of each of four animals with the aim of analysing the distribution of the infused material. After 48 h all four rabbits were killed, and the harvested tibiae were fixed with 10% neutral formalin for 5 days and then decalcified in 20% aqueous EDTA for 4 weeks. Specimens were cut coronally (5 mm thick) for macroscopic photographs and then embedded in paraffin. The embedded sections were then cut coronally (3 μm thick) for microscopic observation.

### Radiological analysis

Soft X-rays of the tibiae were taken using a Model CMB-2T (Softex Co., Kanagawa, Japan). Bone length was measured using SCION Image software.

### Histological analysis

All specimens from the harvested tibiae were fixed with 10% neutral formalin for 5 days, decalcified in 20% aqueous EDTA for 4 weeks and then embedded in paraffin. Sections 3 μm in thickness were cut coronally and stained with haematoxylin and eosin. The numbers of chondrocytes per column in the proliferative (PZ) and hypertrophic (HZ) zones of the GP were counted under a microscope with a 20× objective. All well-orientated "full or intact" cell columns (i.e. columns sectioned in a plane showing consecutive cells extending the entire thickness of each zone) were included in the analysis. The numbers of the cells residing within each zone in these columns were counted, expressed as numbers of cells per column and averaged for each zone of each animal [22]. The total height of the GP was measured as the distance between the two chondrosseous junctions. To measure the heights of the PZ and HZ, their borders were delineated on the basis of morphological criteria [10].

**Table 1** Effect of continuous local infusion of insulin-like growth factor-I (IGF-I) on the length of tibia bone (*NS* not significant)

| Tibia length (mm) | | | | | |
|---|---|---|---|---|---|
| Before infusion | $n$[a] | Duration of infusion (weeks) | Normal saline (N/S) | IGF-I | $p$ value |
| 59.5±0.9 | 5 | One | 67.4±0.4 | 67.4±0.4 | NS |
| 61.7±1.8 | 5 | Two | 73.9±1.6 | 74.9±1.7 | <0.01 |
| 61.1±0.9 | 14 | Four | 88.2±1.4 | 90.3±1.3 | <0.004 |

[a] $n$, Number of animals

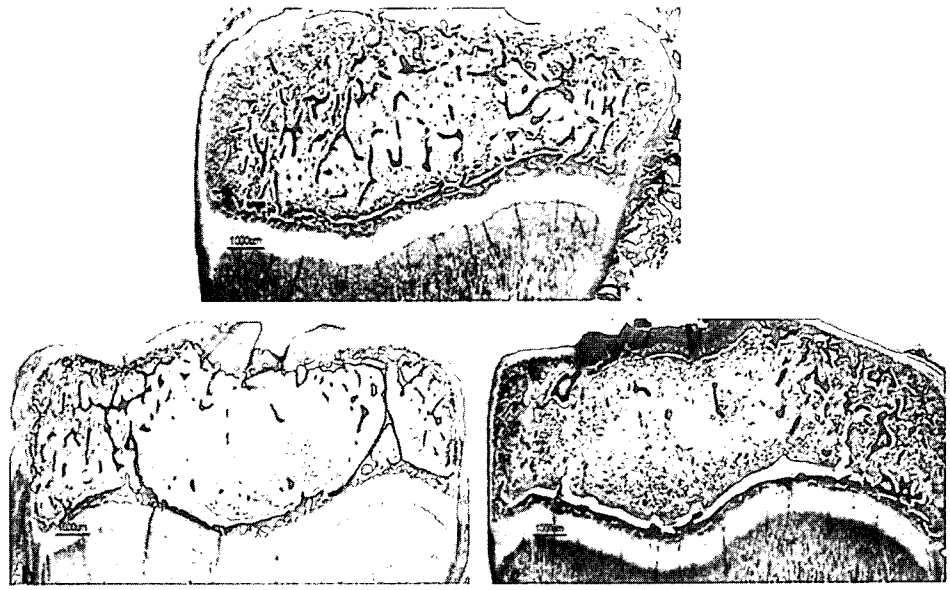

**Fig. 3** Photomicrographs of the proximal tibial epiphysis treated for 4 weeks with IGF-I (a) and N/S (b). Stain: Haematoxylin-eosin. After continuous local infusion of IGF-I, new bone trabeculae were formed in the centre of the epiphysis. In the N/S-treated bone, there was an atrophy of bone trabeculae in the centre of the epiphysis. This atrophy was consistently observed in young rabbits even in intact bone (c)

Peripheral quantitative computerised tomography (pQCT)

Computerised tomography was performed with the Stratec pQCT apparatus (model XCT-960A; Norland/Stratec, Fort Atkinson/Pforzheim, USA/Germany). Metaphyseal pQCT scans of the proximal part of the tibiae were taken to measure trabecular BMD. Measurements were performed on 1-mm-thick slices at 5 mm distal to the proximal growth plate of the tibia.

Statistical analysis

Statistical analysis of the data was performed using Student's paired *t*-test for experimental animals. The results are shown as the mean ± the standard deviation (SD). Values of $p<0.05$ were considered to be significant.

## Results

Skeletal growth

Figure 2 shows a radiograph of IGF-I- and N/S-infused tibiae. After the 2-week infusion of IGF-I locally, the left tibia was approximately 1 mm longer than the right tibia, which had been infused with N/S ($p=0.01$). After the 4-week infusion of IGF-I locally, the left tibia was approximately 2 mm longer than the right tibia, which had been infused with N/S ($p<0.004$). To summarise, after the 2- and 4-week treatments with IGF-I, the length of the left tibia had increased by approximately 1 mm and 2 mm, respectively (Table 1). There was no overgrowth in the fibula of the injected tibiae. There was no difference in the length of the intact tibiae of the control animals and that of the N/S infused tibiae.

Histological analysis

Structures of the epiphysis and adjacent GP were analysed histologically at various stages of the experiment. The intact tibia of a 4-week-old control rabbit showed characteristic histological features, i.e. the bone trabeculae of the epiphysis were thicker and coarser than those of the metaphysis, and the centre of the epiphysis contained only a few bone trabeculae. Intact tibiae of 6- and 8- week-old rabbits showed basically the same histological features, with the exception that the height of the GP had became spontaneously smaller in older animals. When N/S was infused continuously into the epiphysis for 2 or 4 weeks and the histological findings compared with those of age-matched intact tibiae, there was no significant change in the epiphysis and GP (Fig. 3b,c). When IGF-I was infused for 2 weeks or 4 weeks, however, there was a significant increase in the number of bone trabeculae in the centre of the epiphysis (Fig. 3a). In addition, there were significant increases in the height of the GP and in the number of proliferating and hypertrophic chondrocytes in each longitudinal column (Fig. 4a–c; Table 2) in IGF-I treated tibia as compared with N/S-treated tibiae. This result was consistently observed throughout the experiment.

In order to examine the distribution of infused materials, we infused Indian ink – instead of IGF-I – into the proximal epiphysis using the same methodology (osmotic pump). Macroscopically, Indian ink filled up the bone-marrow cavity of the epiphysis (Fig. 5a). Microscopically, some of the dye infiltrated into the GP

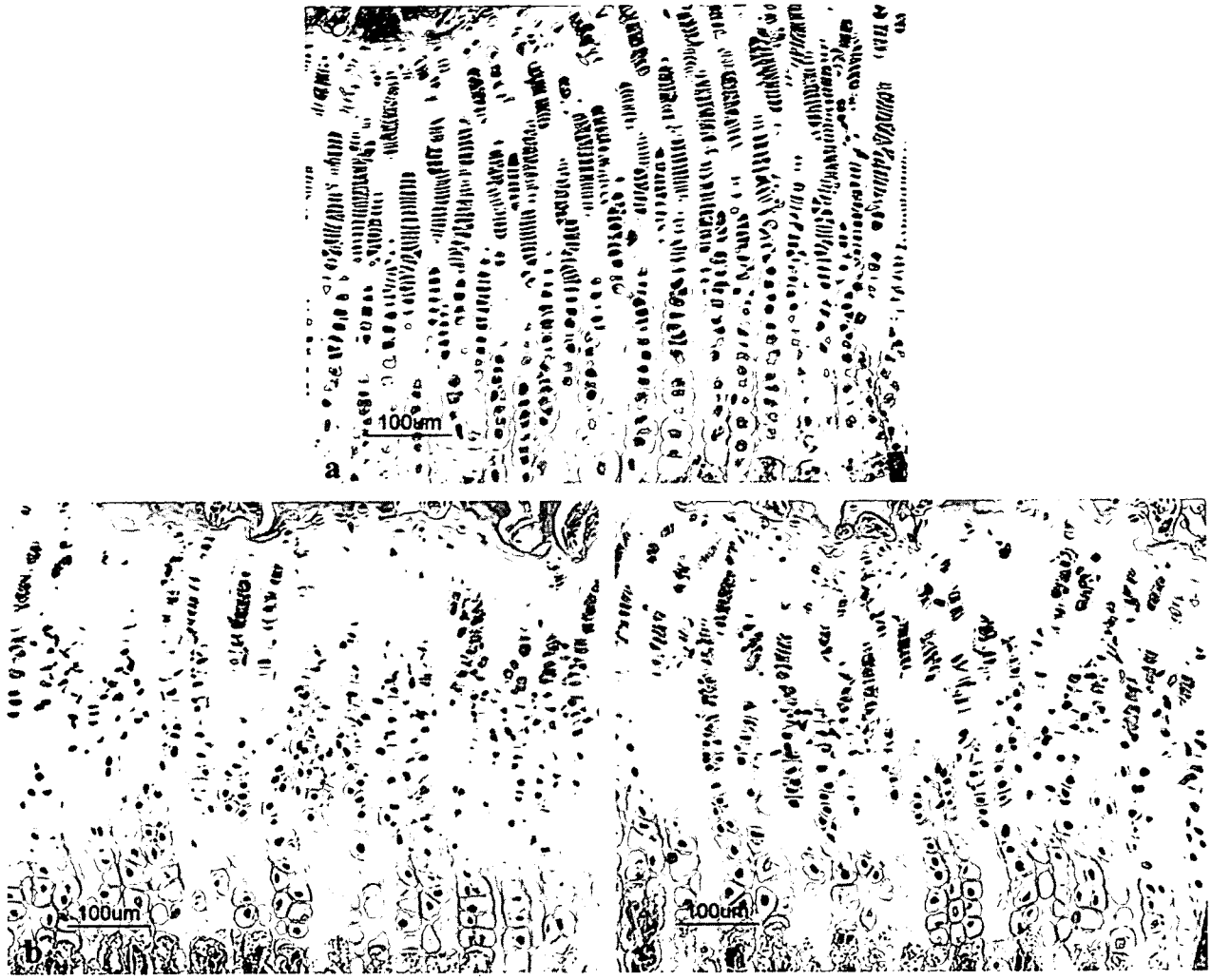


Fig. 4 Photomicrographs of the growth-plates (GPs) treated for 4 weeks with IGF-I (a) and N/S (b). Stain: Haematoxylin-eosin. Continuous local infusion of IGF-I into the epiphysis resulted in a 15% increase in the height of the adjacent GP. Note the significant increase in number of the proliferative (PZ) and hypertrophic (HZ) chondrocytes in each column. c Photomicrographs of the growth plate of the intact tibia. There is no difference between the N/S-treated GP and the intact GP

and stained the proliferating and hypertrophic chondrocytes. The distribution of the Indian ink within the GP was not homogeneous, and an unstained area was distinguishable under low-power magnification. Under high-power magnification, however, the dye reached more or less into the deep layer of the GP. Some of the dye appeared to pass through the GP to reach into the primary spongiosa of the metaphysis (Fig. 5b).

pQCT data

Trabecular volumetric BMD (mg/cm$^3$) of the proximal metaphysis of IGF-I-infused tibiae was significantly higher than that of the control tibiae both in the 2-week group ($p$= 0.012) and 4-week group ($p$<0.001) (Table 3). No significant difference was seen in the 1-week treatment group ($p$=0.18).

## Discussion

We describe herein a method for controlling local bone growth at the level of the individual GP. The continuous infusion of IGF-I into the proximal epiphysis of the tibia promoted longitudinal bone growth: 1 mm in the 2-week treatment and 2 mm in the 4-week treatment. This promotion of bone growth was associated with an increase in the number of bone trabeculae in the epiphysis, an increase in the thickness of the GP, an increase in the number of the proliferating and hypertrophic chondrocytes in each column

**Table 2** Effect of the continuous local infusion of IGF-I on the growth-plate of the proximal tibia (*NS* not significant)

| Experimental groups[a] | N/S | IGF-I | *p* value |
|---|---|---|---|
| One-week group | | | |
| Total height (um) | 714.6±14.9 | 715.6±17.3 | NS |
| RZ height (um) | 78.1±20.6 | 78.5±22.8 | NS |
| PZ height (um) | 382.8±21.9 | 382.8±22.7 | NS |
| PZ cell number | 30.0±1.6 | 30.5±2.4 | NS |
| HZ height (um) | 253.8±12.8 | 254.2±16.5 | NS |
| HZ cell number | 12.0±1.4 | 12.7±0.9 | NS |
| Two-week group | | | |
| Total height (μm) | 549.6±15.2 | 586.9±8.1 | <0.004 |
| RZ height (μm) | 49.9±1.8 | 49.7±1.9 | NS |
| PZ height (μm) | 290.1±15.2 | 316.4±8.1 | <0.017 |
| PZ cell number | 29.6±1.4 | 33.6±1.5 | <0.005 |
| HZ height (μm) | 209.5±5.4 | 220.7±5.4 | <0.023 |
| HZ cell number | 9.4±0.9 | 11.6±0.9 | <0.04 |
| Four-week group | | | |
| Total height (μm) | 511.2±8.4 | 556.6±20.7 | <0.01 |
| RZ height (μm) | 22.5±1.4 | 21.2±1.2 | NS |
| PZ height (μm) | 279.6±8.2 | 304.6±16.9 | <0.03 |
| PZ cell number | 26.8±1.6 | 30.6±0.9 | <0.009 |
| HZ height (μm) | 209.2±3.6 | 230.9±4.9 | <0.003 |
| HZ cell number | 9.4±1.1 | 12.2±1.3 | <0.03 |

[a] RZ, Resting zone; PZ, proliferating zone; HZ, hypertrophic zone. RZ = GP − (PZ + HZ)

and an increase in the BMD and bone mineral content (BMC) of the proximal metaphysis of the tibia bone. Our results are consistent with those of Ohlsson et al., who reported that in the hypophysectomised rat IGF-I increased the width of the epiphyseal GP by increasing the number of proliferating cells [14]. The results of our Indian ink study suggest that locally infused IGF-I mostly stayed within the epiphysis, although a portion did infiltrate into the GP, stimulating the growth and differentiation of physeal chondrocytes. The fibula in the same limb did not show any overgrowth, suggesting that the locally infused IGF-I acted only at the adjacent GP.

IGF-I, also called as somatomedin C, is a single-chain polypeptide of approximately 7.5 kDa that circulates in the plasma at a concentration of 20–80 n*M* in humans [17]. In the original 'somatomedin hypothesis', IGF-I was believed to be a mediator of pituitary GH. Although the mode of action of IGF-I remains open to discussion [20], it has been proposed that the primary effect of GH is to stimulate IGF-I production by the hepatocytes; as such, IGF-I is responsible for stimulating the longitudinal expansion of GPs in an endocrine fashion [3]. More recent work has suggested that GH may act directly on the GP to amplify the production of chondrocytes from germinal zone precursors and then to induce local IGF-I synthesis, which is thought to stimulate the clonal expansion of chondrocyte columns in an autocrine/paracrine manner [13].

The general administration of an over-dose of IGF-I should enhance systemic bone growth and may produce undesirable side effects. For example, high concentrations of serum IGF-I have been shown to be a major risk factor for the development of breast, prostate and colon cancers [4, 6, 15]. We believe that the locally targeted injection of low-dose IGF-I is a more effective and appropriate method to avoid adverse events.

Previous studies in humans and experimental animals [11, 12, 18, 19, 25] have shown that systemic administration of IGF-I enhances not only systemic bone growth but also increases BMD in the metaphysis. There has been no report on the local effect IGF-I on the trabecular bone of the epiphysis and metaphysis. In our study, trabecular volumetric BMD of the proximal metaphysis increased following the continuous infusion of IGF-I into the epiphysis. The exact mechanism by which this effect is achieved is not known, but the Indian ink study suggests the possibility that IGF-I infused into the epiphysis passed through the GP and reached the metaphysis, where it acted on bone formation directly.

In conclusion, we have demonstrated that continuous local infusion of IGF-I into the epiphysis is a valid approach for delivering this protein into the selected GP and to control the growth rate and differentiation of physeal chondrocytes. In our preliminary experiment with this method, IGF-I was the most effective of the various growth factors and cytokines tested (data not shown). In terms of clinical application, this method does not require major surgery because human patients can use an extracorporal pump instead of an osmotic pump. The patients also can avoid osteotomy and the long-term application of a bulky external fixation apparatus. We believe that this method will soon be applied to treat LLD in the field of pediatric orthopaedics.


**Fig. 5** a Frontal section of the proximal tibia after continuous infusion of Indian ink. The bone-marrow cavity of the epiphysis was almost completely filled with the dye. b Photomicrograph (40×) of the GP after continuous infusion of the Indian ink into the epiphysis. The dye infiltrated into the GP and stained the proliferating and hypertrophic chondrocytes. Some of the dye seemed to reach into the primary spongiosa of the metaphysis

**Table 3** Trabecular bone mineral density (mg/cm$^3$) of the proximal metaphysis of the tibiae as measured with peripheral quantitative computerised tomography

| Group | Number | N/S | IGF-I | $p$ value |
|---|---|---|---|---|
| One week | 5 | 92.5±19.6 | 101.4±17.6 | 0.180 |
| Two weeks | 5 | 148.6±36.0 | 164.6±32.2 | <0.012 |
| Four weeks | 14 | 146.0±35.1 | 159.0±35.7 | <0.001 |

**Acknowledgements** This research was supported, in part, by a grant from The Uehara Memorial Foundation 2007. We thank Toshiaki Sano, Department of Human Pathology, The University of Tokushima Graduate School, for his help in preparing the histological sections, Takashi Watanabe, Fuji Memorial Research Institute, Otsuka Pharmaceutical Company for his help in making the bone mineral density measurements and the Fujisawa Chemical Co for the donation of IGF-I.

## References

1. Belthur MV, Bradish CF, Gibbons PJ (2005) Late orthopaedic sequelae following meningococcal septicaemia. A multicentre study. J Bone Joint Surg Br 87:236–240
2. Buckley SL, Smith G, Sponseller PD, Thompson JD, Griffin PP (1990) Open fractures of the tibia in children. J Bone Joint Surg Am 72:1462–1469
3. Daughaday WH, Hall K, Raben MS, Salmon WD Jr, van den Brande JL, van Wyk JJ (1972) Somatomedin: proposed designation for sulphation factor. Nature 235:107
4. Chan JM, Stampfer MJ, Giovannucci E, Gann PH, Ma J, Wilkinson P, Hennekens CH, Pollak M (1998) Plasma insulin-like growth factor-I and prostate cancer risk: a prospective study. Science 279:563–566
5. Grimer RJ, Belthur M, Carter SR, Tillman RM, Cool P (2000) Extendible replacements of the proximal tibia for bone tumours. J Bone Joint Surg Br 82:255–260
6. Hankinson SE, Willett WC, Colditz GA, Hunter DJ, Michaud DS, Deroo B, Rosner B, Speizer FE, Pollak M (1998) Circulating concentrations of insulin-like growth factor-I and risk of breast cancer. Lancet 113:1393–1396
7. Herring JA, Tachdjian MO (2002) Tachdjian's pediatric orthopaedics, vol. 2, 3rd edn. Saunders, Philadelphia, pp 1058–1095
8. Hunziker EB, Wagner J, Zapf J (1994) Differential effects of insulin-like growth factor I and growth hormone on developmental stages of rat growth plate chondrocytes in vivo. J Clin Invest 93:1078–1086
9. Kojimoto H, Yasui N, Goto T, Matsuda S, Shimomura Y (1988) Bone lengthening in rabbits by callus distraction. The role of periosteum and endosteum. J Bone Joint Surg Br 70:543–549
10. Lupu F, Terwilliger JD, Lee K, Segre GV, Efstratiadis A (2001) Roles of growth hormone and insulin-like growth factor 1 in mouse postnatal growth. Dev Biol 229:141–162
11. Mohan S, Richman C, Guo R, Amaar Y, Donahue LR, Wergedal J, Baylink DJ (2003) Insulin-like growth factor regulates peak bone mineral density in mice by both growth hormone-dependent and -independent mechanisms. Endocrinology 144:929–936
12. Mueller K, Cortesi R, Modrowski D, Marie PJ (1994) Stimulation of trabecular bone formation by insulin-like growth factor I in adult ovariectomized rats. Am J Physiol 267:E1–E6
13. Ohlsson C, Bengtsson BA, Isaksson OG, Andreassen TT, Slootweg MC (1998) Growth hormone and bone. Endocr Rev 19:55–79
14. Ohlsson C, Nilsson A, Isaksson O, Lindahl A (1992) Growth hormone induces multiplication of the slowly cycling germinal cells of the rat tibial growth plate. Proc Natl Acad Sci USA 89:9826–9830
15. Palmqvist R, Hallmans G, Rinaldi S, Biessy C, Stenling R, Riboli E, Kaaks R (2002) Plasma insulin-like growth factor I, insulin-like growth factor binding protein 3, and risk of colorectal cancer: a prospective study in northern Sweden. Gut 50:642–646

16. Reynolds DA (1981) Growth changes in fractured long-bones: a study of 126 children. J Bone Joint Surg Br 63:83–88
17. Rosen CJ (1999) Serum insulin-like growth factors and insulin-like growth factor-binding proteins: clinical implications. Clin Chem 45–48:1384–1390
18. Spencer EM, Liu CC, Si EC, Howard GA (1991) In vivo actions of insulin-like growth factor-I (IGF-I) on bone formation and resorption in rats. Bone 12:21–26
19. Wakisaka A, Tanaka H, Barnes J, Liang CT (1998) Effect of locally infused IGF-I on femoral gene expression and bone turnover activity in old rats. J Bone Miner Res 13:13–19
20. Wang J, Zhou J, Bondy CA (1999) Igf1 promotes longitudinal bone growth by insulin-like actions augmenting chondrocyte hypertrophy. Faseb J 13–14:1985–1990
21. Woods KA, Camacho-Hubner C, Savage MO, Clark AJ (1996) Intrauterine growth retardation and postnatal growth failure associated with deletion of the insulin-like growth factor I gene. N Engl J Med 335:1363–1367
22. Xian CJ, Howarth GS, Cool JC, Foster BK (2004) Effects of acute 5-fluorouracil chemotherapy and insulin-like growth factor-I pretreatment on growth plate cartilage and metaphyseal bone in rats. Bone 35:739–749
23. Yasui N, Sato M, Ochi T, Kimura T, Kawahata H, Kitamura Y, Nomura S (1997) Three modes of ossification during distraction osteogenesis in the rat. J Bone Joint Surg Br 79:824–830
24. Yasui N, Kojimoto H, Sasaki K, Kitada A, Shimizu H, Shimomura Y(1993) Factors affecting callus distraction in limb lengthening. Clin Orthop 293:55–60
25. Zhao G, Monier-Faugere MC, Langub MC, Geng Z, Nakayama T, Pike JW, Chernausek SD, Rosen CJ, Donahue LR, Malluche HH, Fagin JA, Clemens TL (2000) Targeted overexpression of insulin-like growth factor I to osteoblasts of transgenic mice: increased trabecular bone volume without increased osteoblast proliferation. Endocrinology 141:2674–2682

# Minimally Invasive Endoscopic Removal of a Herniated Nucleus Pulposus that had Migrated to the S1 Nerve Root Foramen

**Author** I. Tonogai, K. Sairyo, K. Higashino, T. Sakai, S. Katoh, N. Yasui

**Affiliation** Department of Orthopedics, The University of Tokushima School of Medicine, Tokushima, Japan

**Key words**
- endoscopic surgery
- migrated HNP
- radiculopathy

## Abstract

In this report, we described an adult case with a lumbar herniated nucleus pulposus that had migrated to the S1 nerve root foramen from L5-S1 disc space. Endoscopically, the migrated mass was successfully removed after laminectomy at the S1 with a small skin incision of 20 mm in length. Unlike the other levels, the intraforaminally migrated mass along the S1 root can be excised without any removal of the facet joints; therefore, additional spinal fusion is not necessary. Thus, an S1 foraminal migrated mass can be a good surgical candidate for minimally invasive endoscopic surgery.

## Introduction

Recently, a minimally invasive technique for lumbar decompression surgery has been developed [1–7]. Intraforaminally migrated disc herniation is a rare herniation of the nucleus pulposus. Among those cases, migration into an S1 nerve root foramen is even rarer, since herniation of the nucleus pulposus at L5-S1 is likely to migrate into an L5 nerve root foramen.

The migrated herniation mass can be removed using a spinal endoscope [7]; however, that was not as easy as the endoscopic removal of herniation at the disc level (standard condition). To remove the migrated mass, an additional laminotomy was necessary and the tubular retractor needed to be appropriately moved during the operation.

In the literature, there are no case reports of the endoscopic removal of an intraforaminally migrated disc herniation. We present the case of a patient with an intraforaminally migrated disc herniation, which was successfully removed using a spinal endoscope.

## Case report

The patient, a 40-year-old man, felt acute low back pain when carrying a heavy baggage at work. He also experienced strong paresthesic burning pain radiating to the plantar and lateral sides of the right leg. He was unable to walk because of the pain. Although his low back pain slightly decreased with rest, the strong burning pain and paresthesia in the right leg persisted. Thus, he could not work.

He visited a local hospital, where MRI revealed a herniated nucleus pulposus on the right side at the L5-S1 level. **Fig. 1** shows the MRIs taken at the hospital. The herniated mass spread along the right S1 nerve root (left pictures in **Fig. 1**) and migrated to the caudal side. **Fig. 2** shows the axial section from L5-S1 to the sacrum. Each white arrow in the axial sections indicates the herniated mass. In the right S1 nerve root foramen seen on the axial picture through the middle of the S1 body, the herniated mass was observed compressing the nerve root. The patient was first treated conservatively. However, his symptoms gradually worsened, and he noted weakness of the right ankle.

Then he was referred to our Orthopedic Department because of the approximately 1-month-long course of right leg pain and was admitted for surgery. The straight leg raising test (SLRT) was positive at 70 degrees on the right side and weakness of the right flexor hallucis longus with 4/5 on manual muscle testing (MMT) was noted. The neurological examination revealed paresthesia and decreased sensation along the right S1 dermatome. The findings indicated right S1 radiculopathy and were in good agreement with MRI findings, i.e., compression of the S1 nerve

**Bibliography**
**DOI** 10.1055/s-2007-982510
Minim Invas Neurosurg 2007; 50: 173–177

ISSN 0946-7211

**Correspondence**
***K. Sairyo, MD, PhD***
Department of Orthopedics
The University of Tokushima
3-18-15, Kuramoto
770-8503 Tokushima
Japan
Tel.: +81/88/633 72 40
Fax: +81/88/633 01 78
sairyokun@hotmail.com

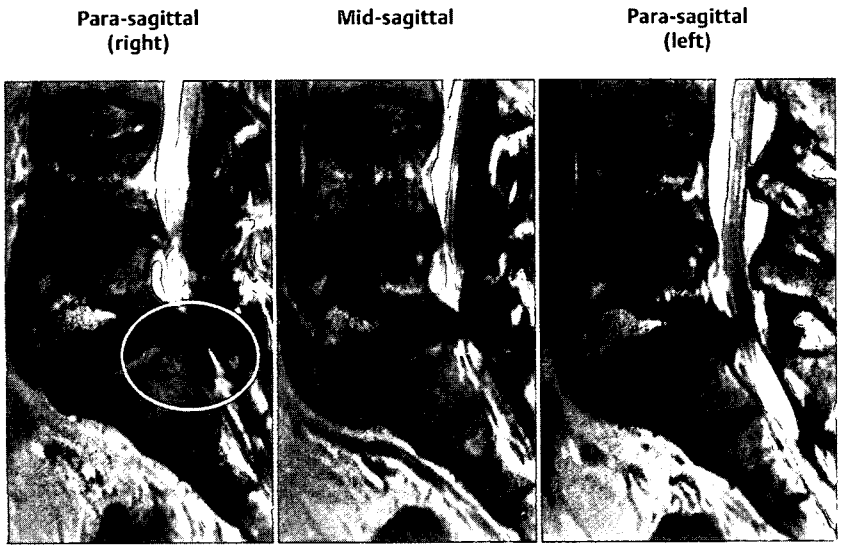


Fig. 1 Sagittal MRIs taken before surgery.

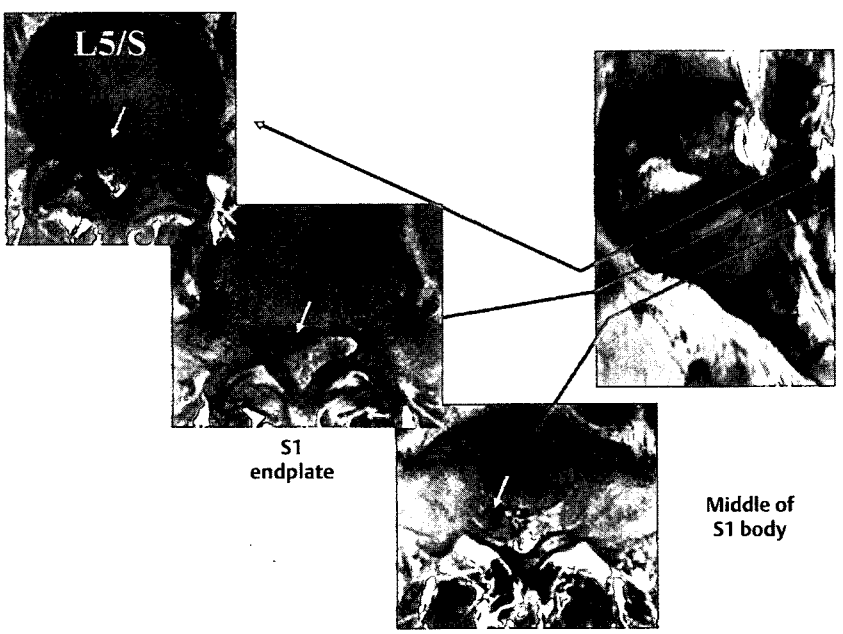


Fig. 2 Axial MRIs taken before surgery.

root by an intraforaminally migrated lumbar disc herniation from the L5-S1 disc. The migrated mass probably compressed the dorsal root ganglion, because he had a strong paresthesic sensation in his right foot. Although MRI showed slight bulging of the disc at L4/5 as well, the neurological deficit such as weakness and paresthesia were only found at the S1 nerve root level. Thus, we decided to remove the intraforaminally migrated disc material at the S1 foramen.

An endoscopic excision of the herniated mass, after right L5-S1 laminotomy and decompression of the right S1 root with a 20 mm skin incision, were performed. ○ **Fig. 3** shows the skin incision scar in this patient (1 finger breadth incision in length). After the incision, laminotomy of L5 and un-roofing of S1 nerve root (selective laminotomy) were performed using a Kerrison rongeur. ○ **Fig. 4** shows the laminectomized area. Please note the area of removal of the S1 lamina. The dura matter and S1 nerve root were then exposed. The S1 root nerve was found to be tightly compressed at the disc level (○ **Fig. 5**). The herniated mass at the L5-S1 intervertebral disc level was removed; however, the mobility of the S1 root did not improve. The migrated HNP was inspected along the S1 nerve root into the foramen. The caudally migrated herniation mass was detected at the caudal portion toward the S1 foramen at the S1 pedicle level (○ **Fig. 6**). The herniation was successfully removed endoscopically without any complications. The operation lasted 150 minutes, and there was little blood loss. ○ **Fig. 7** demonstrates the MRIs after the surgery. Note the migrated mass is removed and the S1 nerve root is decompressed.

After the operation the patient experienced a dramatic resolution of symptoms, with a 5/5 FHL on the MMT. His pain disappeared completely, as did his muscle weakness and paresthesia. He could start walking smoothly the day after surgery and showed a complete relief of pain. No recurrence was noted at the last follow-up.

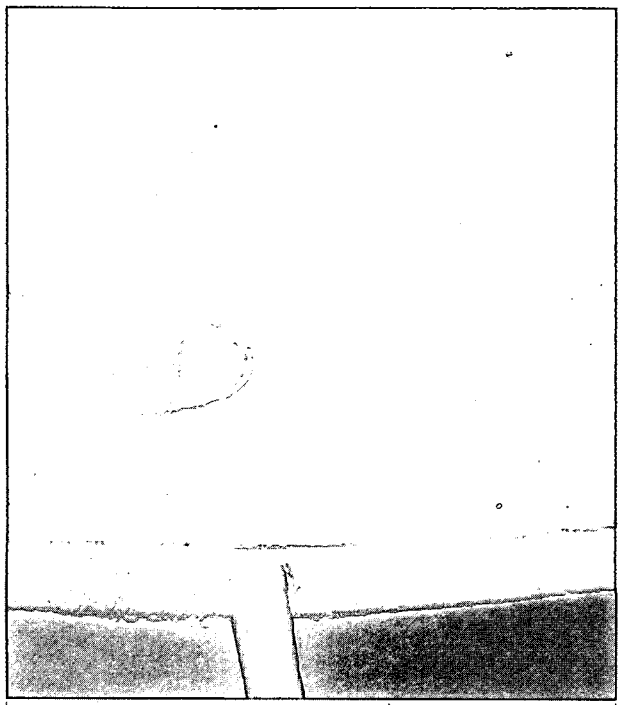

**Fig. 3** Operation scar.

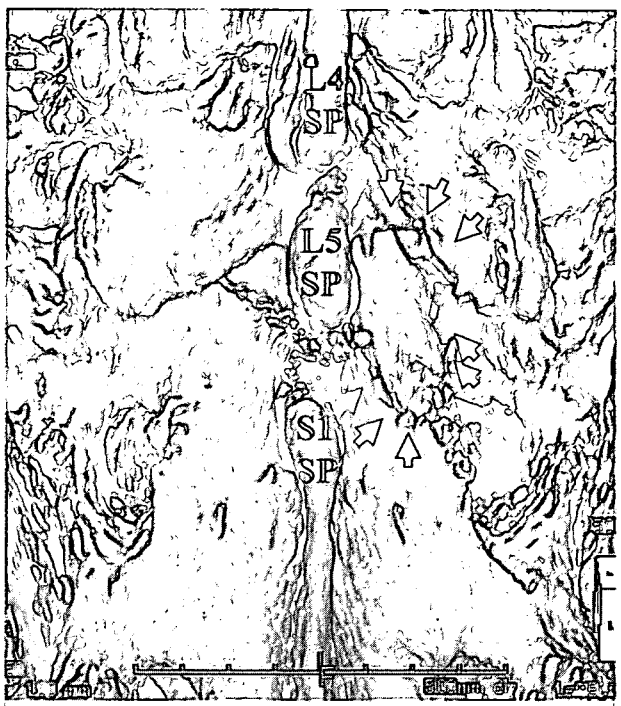


**Fig. 4** Posterior view of 3D CT. Note the laminectomized area.

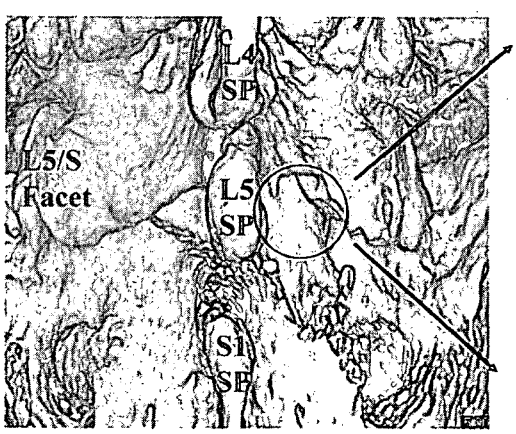


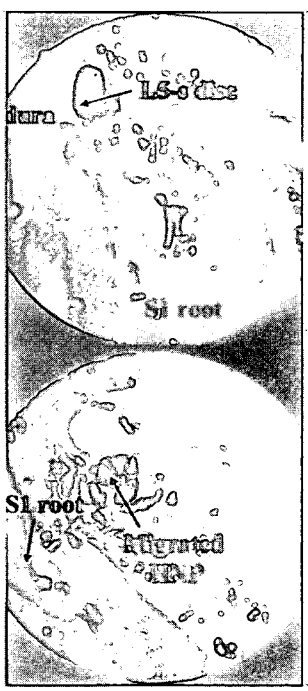


**Fig. 5** Endoscopic view at the L5-S1 disc level.

## Discussion

This minimally invasive endoscopic technique was first reported by Foley and Smith [1]. Huang et al. [8] and Sasaoka et al. [9] stated that endoscopic posterior decompression surgery was less invasive than the conventional open surgery based on data of IL-6 and CRP after the surgery. Biomechanically, endoscopic surgery was also reported to be minimally invasive [10]. Muscle injuries related to this endoscopic technique were investigated and compared to those related to conventional open surgery. Ikawa et al. [11] investigated back muscle injuries after MED surgery using near infrared spectroscopy (NIRS), and showed that the MED technique was not associated with an alteration of hemodynamics after the surgery, as observed after conventional open surgery. Thus, the number of lumbar disorders that can be treated using the minimally invasive endoscopic technique will increase in the future.

Recently, the technique has been applied to treat lumbar spondylolysis, cervical radiculopathy, lumbar cystic lesions, and lumbar lateral stenosis [1–7, 12].

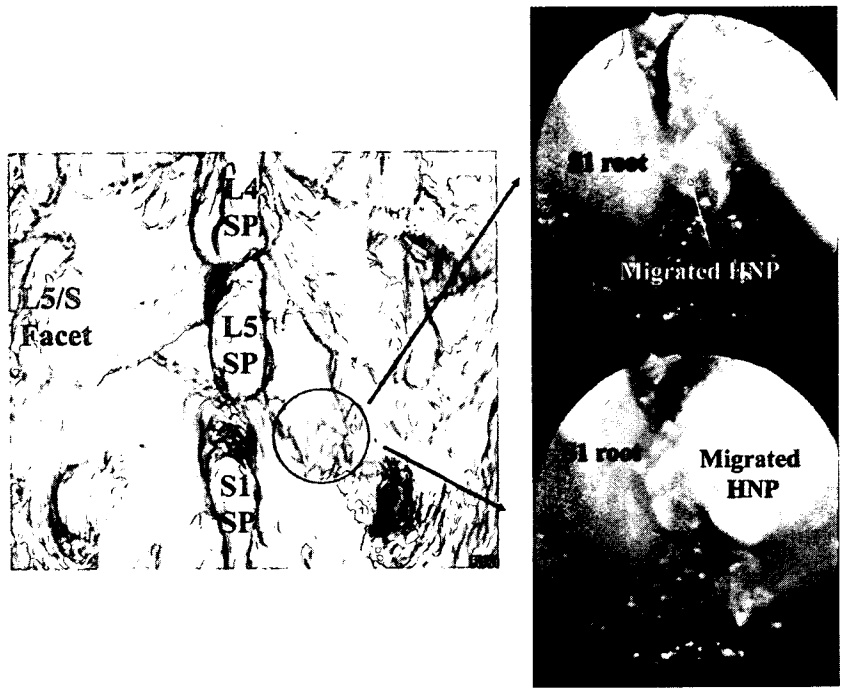


**Fig. 6** Endoscopic view of the S1 nerve root foramen.

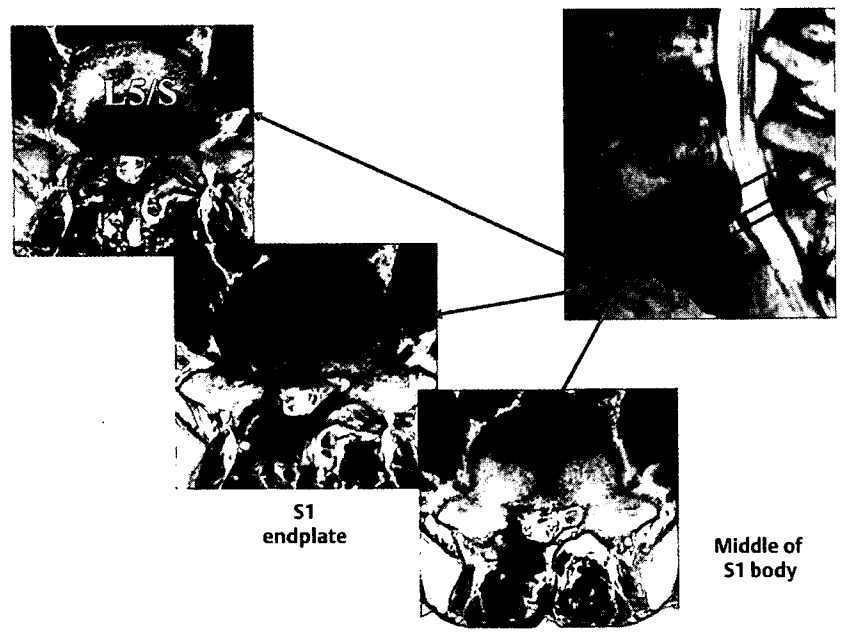


**Fig. 7** Axial MRI taken after surgery.

In this report, we describe the case of a patient who underwent endoscopic removal of an intraforanimally migrated herniated nucleus pulposus. The mass was successfully removed endoscopically. Compared to surgery for an ordinary herniated mass at the disc level, the laminectomized area was large (○ **Fig. 4**). However, by appropriately changing the position of the tubular retractor, it was not technically difficult to endoscopically laminectomize such an area (○ **Fig. 3**).

The intraforaminally migrated mass along the S1 root can be excised without any removal of the facet joints; therefore, additional spinal fusion is not necessary. However, at other levels, such as L3-4 and L4-5, additional facetectomy is sometimes required to access a migrated intraforaminal mass. Thus, an S1 foraminal migrated mass can be a good surgical candidate for minimally invasive endoscopic surgery.

## References

1 *Foley KT, Smith MM.* Microendoscopic discectomy. Techniques in Neurosurgery 1997; 3: 301–307
2 *Sairyo K, Katoh S, Sakamaki T et al.* A new endoscopic technique to decompress lumbar nerve roots affected by spondylolysis. Technical note. J Neurosurg 2003; 98 (3 Suppl):290–293
3 *Ishii K, Matsumoto M, Watanabe K et al.* Endoscopic resection of cystic lesions in the lumbar spinal canal: a report of two cases. Minim Invas Neurosurg 2005; 48: 240–243
4 *Matsumoto M, Chiba K, Ishii K et al.* Microendoscopic partial resection of the sacral ala to relieve extraforaminal entrapment of the L-5 spinal nerve at the lumbosacral tunnel. Technical note. J Neurosurg Spine 2006; 4: 342–346

5 *Inui A, Sairyo K, Katoh S et al.* Endoscopic resection of lumbar extruded osseous endplate causing radiculopathy. Minim Invas Neurosurg 2006; 49: 55–57
6 *Sairyo K, Goel VK, Biyani A et al.* Decompression surgery for lumbar spondylolysis without fusion: A review article. Internet J Spine Surg 2006; 2
7 *Nakagawa Y, Yoshida M, Maia K.* Microendoscopic discectomy (MED) for surgical management of lumbar disc disease. Internet J Spine Surg 2006; 2
8 *Huang TJ, Hsu RW, Li YY et al.* Less systemic cytokine response in patients following microendoscopic versus open lumbar discectomy. J Orthop Res 2005; 23: 406–411
9 *Sasaoka R, Nakamura H, Konishi S et al.* Objective assessment of reduced invasiveness in MED compared with conventional one-level laminotomy. Eur Spine J 2006; 15: 577–582
10 *Sairyo K, God VK, Masuda A et al.* Biomechanical rationale of endoscopic decompression for lumbar spondylolysis as an effective minimally invasive procedure – a study based on the finite element analysis. Minim Invas Neurosurg 2005; 48: 119–122
11 *Ikawa M, Atsuta Y, Tsunekawa H, Matsuno T.* Is MED less invasive than LOVE? Examination to the influence on PVM by using near infrared spectroscopy. Jpn J Spine Research Society 2004; 15: 242
12 *Yabuki S, Kikuchi S.* Endoscopic partial laminectomy for cervical myelopathy. J Neurosurg Spine 2005; 2: 170–174

THE JOURNAL OF BONE & JOINT SURGERY (BRITISH)

# Callus formation during healing of the repaired tendon-bone junction

## A RAT EXPERIMENTAL MODEL

N. Hibino,
Y. Hamada,
K. Sairyo,
K. Yukata,
T. Sano,
N. Yasui

*From University of Tokushima Graduate School, Tokushima, Japan*

**This study was undertaken to elucidate the mechanism of biological repair at the tendon-bone junction in a rat model. The stump of the toe flexor tendon was sutured to a drilled hole in the tibia (tendon suture group, n = 23) to investigate healing of the tendon-bone junction both radiologically and histologically. Radiological and histological findings were compared with those observed in a sham control group where the bone alone was drilled (n = 19). The biomechanical strength of the repaired junction was confirmed by pull-out testing six weeks after surgery in four rats in the tendon suture group. Callus formation was observed at the site of repair in the tendon suture group, whereas in the sham group callus formation was minimal. During the pull-out test, the repaired tendon-bone junction did not fail because the musculotendinous junction always disrupted first.**

**In order to understand the factors that influenced callus formation at the site of repair, four further groups were evaluated. The nature of the sutured tendon itself was investigated by analysing healing of a tendon stump after necrosis had been induced with liquid nitrogen in 16 cases. A proximal suture group (n = 16) and a partial tenotomy group (n = 16) were prepared to investigate the effects of biomechanical loading on the site of repair. Finally, a group where the periosteum had been excised at the site of repair (n = 16) was examined to study the role of the periosteum. These four groups showed less callus formation radiologically and histologically than did the tendon suture group.**

**In conclusion, the sutured tendon-bone junction healed and achieved mechanical strength at six weeks after suturing, showing good local callus formation. The viability of the tendon stump, mechanical loading and intact periosteum were all found to be important factors for better callus formation at a repaired tendon-bone junction.**

N. Hibino, MD, Orthopaedic Surgeon
Y. Hamada, MD, PhD, Assistant Professor
K. Sairyo, MD, PhD, Associate Professor
K. Yukata, MD, Orthopaedic Surgeon
N. Yasui, MD, PhD, Professor
Department of Orthopaedics
T. Sano, MD, PhD, Professor
Department of Human Pathology
University of Tokushima, 3-18-15, Kuramoto, Tokushima 770-8503, Japan.

Correspondence should be sent to Professor N. Yasui; e-mail: nyasui@clin.med.tokushima-v.ac.jp


doi:10.1302/0301-620X.89B11.19847 $2.00

*J Bone Joint Surg [Br]* 2007;89-B:1539-44.
*Received 21 June 2007; Accepted 20 July 2007*

Tendons and ligaments are usually treated surgically when injured at the site of insertion into bone. Various techniques are used to attach tendon to bone, such as an endobutton, a suture anchor and an interference screw.[1] In order to achieve good long-term results, biological integration between the tendon and bone is required.

The normal tendon-bone junction is a unique structure composed of four zones, including a transitional fibrocartilaginous zone characterised by the presence of calcified fibrocartilage next to the bone and non-calcified fibrocartilage next to the tendon.[2,3] There is controversy about whether these four zones are restored at the repaired tendon-bone junction.[4-6] In previous studies the healing of tendon-to-bone has been examined in dogs or rabbits both histologically and biomechanically.[7,8] However, radiological evaluation was not undertaken and this is essential to assess the integration of tendon-to-bone.

We have attempted to clarify the mechanism of tendon-bone healing using a suture anchor technique in a rat model and assessing callus formation by radiological and histological examination.

## Materials and Methods

We obtained 106 seven-week-old male Wistar rats (Charles River Japan Co. Ltd, Yokohama, Japan), weighing 280 g to 300 g. The rats were housed in individual cages, at 23°C and a humidity of 55% in a controlled room under a 12:12 hour light-dark cycle. The animals had free access to food and water. This study protocol conformed to the guidelines for the care and use of laboratory animals of our university. The rats were divided into groups (Table I).

**Study I: healing process.** Each rat was anaesthetised with sodium pentobarbital (50 mg/kg body-weight) and a longitudinal skin incision was made on the medial aspect of the tibia. A

**Table I.** Number of rats used for each experiment

| | Tendon suture group | Control group | Each group for study II | Total for study II | Total |
|---|---|---|---|---|---|
| Radiological studies | 10 | 10 | 7 | 28 | 48 |
| Histological analysis | | | | | |
| 1 week | 3 | 3 | 3 | 12 | 18 |
| 3 weeks | 3 | 3 | 3 | 12 | 18 |
| 6 weeks | 3 | 3 | 3 | 12 | 18 |
| Biomechanical study | 4 | 0 | 0 | 0 | 4 |
| Total | 23 | 19 | 16 | 64 | 106 |

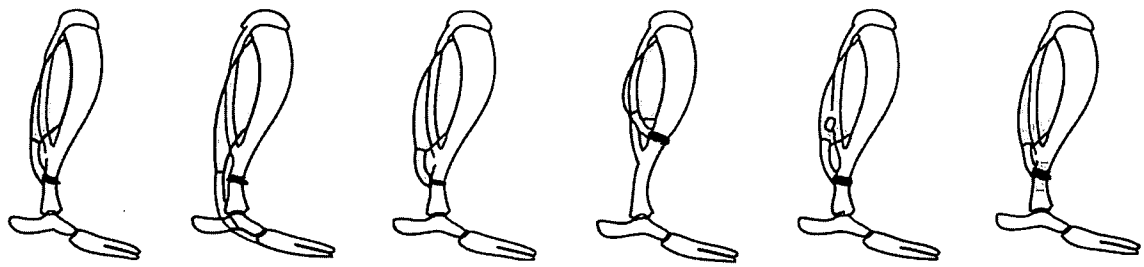

Fig. 1a Fig. 1b Fig. 1c Fig. 1d Fig. 1e Fig. 1f

The experimental groups: a) tendon suture group (n = 23), b) control group (n = 19), c) necrosis group (n = 16), d) proximal suture group (n = 16), e) partial tenotomy group (n = 16), and f) periosteal excision group (n = 16).

hole 1.0 mm in diameter was drilled across the width of the distal third of the tibia perpendicular to the long axis of the bone, distal to the distal tibiofibular junction. The flexor digitorum fibularis tendons (toe flexors) were divided at the medial aspect of the ankle. We introduced a core suture using the Kessler method[9] into the stump of the tendon using a 5/0 nylon suture which was passed through the hole and fixed on the anterior aspect of the tibia (tendon suture group: n = 23; Fig. 1a). As a control, a sham-operative group was prepared. A hole 1.0 mm in diameter was drilled in the tibia as before and a 5/0 nylon thread was passed through it and fixed without invading the flexor tendons (control group: n = 19; Fig. 1b).

*Radiological analysis.* The amount of callus formed was assessed on lateral radiographs at one, three and six weeks after operation. The area of the callus was measured using the National Institutes of Health (NIH) Image Software, version 1.6 (Bethesda, Maryland).

*Histological analysis.* At one, three and six weeks after the operation 54 rats were killed and the tibia was harvested for histological examination of the tendon-bone interface. The specimen was fixed in 10% buffered formalin before being decalcified in ethylenediamethyl-acetic acid (EDTA) and embedded in paraffin. Sections of 5 μm thickness were obtained in the axial plane from the bone tunnel. The sections were stained with haematoxylin and eosin and examined under a light microscope. The histological evaluation was performed by three different researchers (NH, YH, KY).

*Biomechanical analysis.* In order to investigate mechanical healing at the tendon-bone junction in the tendon suture group, we concluded a pull-out test with four examples. Immediately after the specimen was harvested, it was stored at -80°C prior to thawing to room temperature over one day before the testing. With a vice clip, the tibia was secured to the base plate of an AC servo hydraulic materials testing system (AGS-100D, Shimadzu, Kyoto, Japan) and the muscle belly of the sutured flexor digitorum fibularis was held at the actuator. The actuator was moved vertically at a speed of 5 mm/min to distract the muscle-tendon-bone complex until failure. The ultimate strength at failure (N) and the site of failure were confirmed.

**Study II: factors influencing callus formation.** In order to clarify the role of the tendon stump, mechanical stress and periosteum in callus formation at the repaired tendon-bone junction, animals were allocated to four additional groups.

*Role of the tendon stump in callus formation.* We induced necrosis of the tendon stump by soaking it in liquid nitrogen for one minute[10] and then sutured it to the hole in the bone (necrosis group, n = 16; Fig. 1c).

Fig. 2a

Fig. 2b

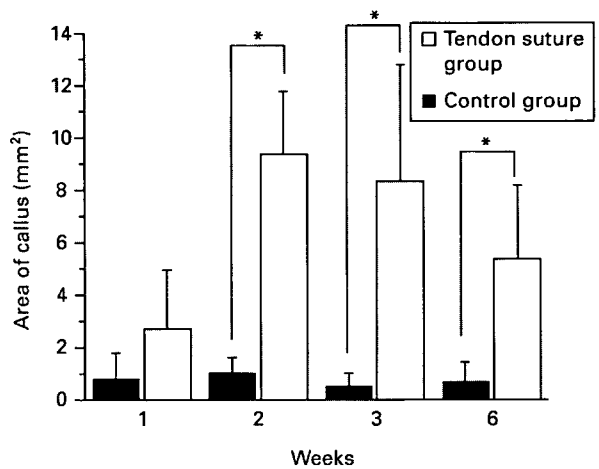


Fig. 2c

Serial radiological changes in a) the tendon suture group and b) the control group. c) Serial changes in the amount of callus in the tendon suture group and in the control group (*, $p < 0.05$ using the *post hoc* analysis with Tukey-Kramer test).

*Role of traction force (mechanical loading) in callus formation.* In order to reduce mechanical loading through the sutured tendon we sutured its stump at a site proximal to the standard position of the tibiofibular junction (proximal suture group, n = 16; Fig. 1d). For the same purpose we created a partial tenotomy at the muscle-tendon junction prior to reattaching the tendon at the standard position used in the tendon suture group (partial tenotomy group, n = 16; Fig. 1e).

*Role of periosteum in callus formation.* We removed 1 $cm^2$ of periosteum around the centre of the drill-hole in the tibia prior to suturing the tendon stump to the hole in the bone (periosteal excision group, n = 16; Fig. 1f).

Except for the specimens used for the biomechanical assessment the same histological and radiological analyses undertaken in the first stage of the study were conducted to evaluate the subsequent callus formation. In all cases the limbs were not immobilised and the rats were allowed to move freely after the operation.

**Statistical analysis.** Statistical differences were evaluated using one-way analysis of variance (ANOVA) and a *post hoc* analysis with the Tukey-Kramer test. A p-value $< 0.05$ was regarded as statistically significant.

## Results

### Study I: healing process

*Radiographs.* In the tendon-bone suture group, the large cartilaginous callus observed at the site of the repair two weeks after surgery gradually remodelled, decreasing in size by six weeks when the bony prominence at the tendon-bone interface was still present (Fig. 2a). There was little callus formation in the control group (Fig. 2b). The area of callus in the control group was significantly smaller than in the tendon suture group (*post hoc* analysis with Tukey-Kramer test, $p < 0.05$) (Fig. 2c).

*Histological analysis.* The histological findings in each group corresponded well with the radiological appearances. In the tendon suture group, serial histological changes revealed callus formation at the tendon-bone interface. During the first week, granulation tissue at the site of repair was initially composed of inflammatory cells. Intramembranous ossification around the whole tibia took

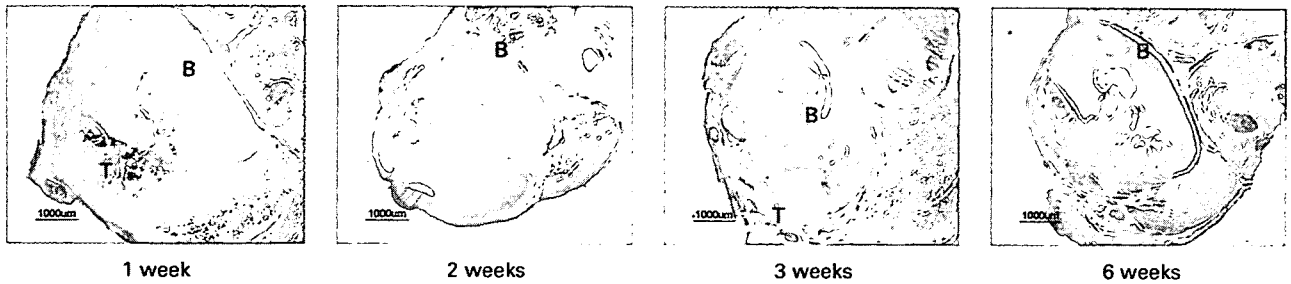


Fig. 3a

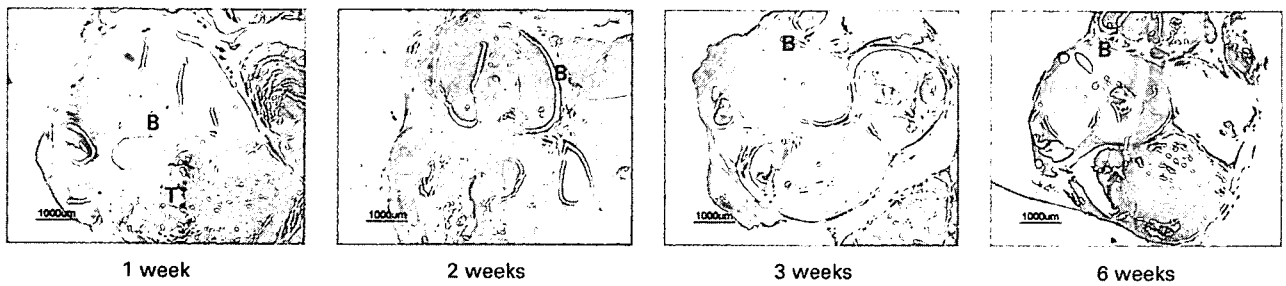


Fig. 3b

Serial histological changes in haematoxylin and eosin-stained sections of the axial plane through the bone tunnel in a) the tendon suture group and b) the control group. T, tendon stump; B, drill-hole in bone (all sections: magnification × 2; scale, bar, 1000 μm).

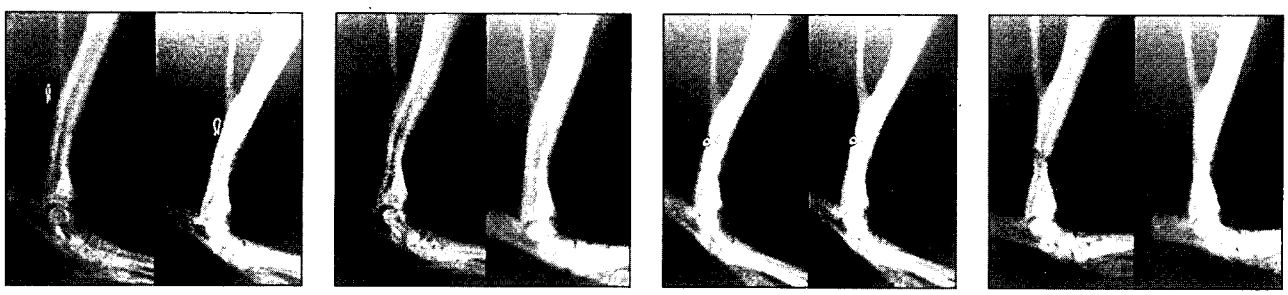

Fig. 4a Fig. 4b Fig. 4c Fig. 4d

Radiological changes at three (left side) and six (right side) weeks after the operation, in a) the necrosis group, b) proximal suture group, c) partial tenotomy group, and d) periosteal excision group.

place under the periosteum without the formation of an intermediate cartilaginous layer (Fig. 3a). By three weeks, woven bone was found on the posterior aspect of the tibia at the transitional tendon-to-bone zone with an intermediate cartilaginous layer. Some chondrocytes began to calcify the surrounding matrix, resembling the endochondral ossification found in fracture healing. By six weeks, the woven bone within the intermediate cartilaginous layer was replaced by lamellar bone (Fig. 3a).

There was little callus formation in the hole in the bone in the control group (Fig. 3b). Intramembranous ossification took place under the periosteum.

*Biomechanical analysis.* At six weeks after the operation, the muscle-tendon-bone complex failed in all four specimens at the muscle-tendon junction at a mean of 28.8 N (26.60 to 29.35). The sutured tendon-bone junction did not break during the pull-out test.

## Study II: factors influencing callus formation

*Role of the tendon stump in callus formation.* The radiographs show that callus formation was reduced in the necrosis group (Fig. 4) compared with that in the tendon suture group (Fig. 2a).

*Role of traction force.* The formation of callus was reduced in the proximal suture and partial tenotomy groups compared with that in the tendon suture group (Fig. 4).

*Role of the periosteum.* Periosteal excision markedly compromised callus formation (Fig. 4).

The area of callus in each group at three weeks after the operation is demonstrated in Figure 5. Without either mechanical load or the biological effect from the tendon

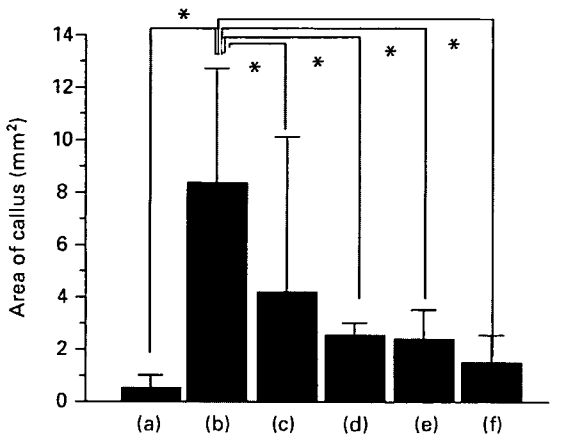


Fig. 5

Barchart showing mean and standard deviation area of callus at three weeks after the operation a) the control group, b) tendon suture group, c) proximal suture group, d) partial tenotomy group, e) necrosis group, and f) periosteal excision group (*, *post hoc* analysis with the Tukey-Kramer test, $p < 0.05$).

stump, callus formation at the site of tendon-bone repair was significantly reduced (*post hoc* analysis with Tukey-Kramer test, $p < 0.05$) compared with that in the tendon suture group; however, callus formation was even less in the control group (*post hoc* with Tukey-Kramer test, $p < 0.05$).

Histological analysis in the necrosis group showed that minimal callus formation was induced at the repaired tendon-bone junction (Fig. 6). Similarly when the traction at the tendon reattachment had been reduced by suturing in a proximal position or by partial tenotomy, callus formation was poor three weeks after the operation (Fig. 6).

In the absence of periosteum the formation of an external callus at the repaired tendon-bone junction was also deficient (Fig. 6).

## Discussion

In our model, the tendon-bone junction was mechanically healed six weeks after surgery and was confirmed by the point of reattachment being mechanically stronger than that of the muscle-tendon junction. Radiologically, we found a large amount of callus formed at the suture site during normal healing. At the tendon-bone junction, callus was also confirmed histologically, but the typical four-zone structure of the junction was not observed.

Previously, it has been reported that the junction healed showing the normal transitional four-zone structure.[4-6] However, the importance of these four zones for the repair process is still a matter of controversy.[4-6] Leung et al[6] histologically investigated the repaired tendon-bone junction up to 24 weeks after surgery. They found that the structural integration at the site of repair was poor without a typical intermittent fibrocartilage zone, suggesting that the four-zone structure may not be important to obtain good healing. Our results were similar.

Instead of obtaining the four zones during healing, we found that callus formed at the site of normal healing and presume that callus formation is a key factor for healing. For appropriate callus formation in the second part of our study we showed that the viability of the tendon stump, mechanical loading and the presence of periosteum were important.

It has been widely recognised[11] that cell proliferation and differentiation, the presence of a number of growth factors and an intact scaffold greatly contribute to tissue regeneration. As there was little callus formation in the control group, the presence of the tendon stump seemed to be important for the stimulation of callus at the tendon-bone interface. This was tested by preparing a tendon stump necrosis group. Consistent with our hypothesis, callus formation was minimal in this group compared with the normal tendon suture group, suggesting that the tendon stump may release factors related to osteogenesis.

In general, mechanical stress is a key factor for osteogenesis. This principle has been seen to operate in our study because in both groups where the loading was reduced, the callus formation was poor.

Kojimoto et al[12] found that preservation of the periosteum was important for callus formation in bone lengthening in a rabbit model of callus distraction. In a clinical

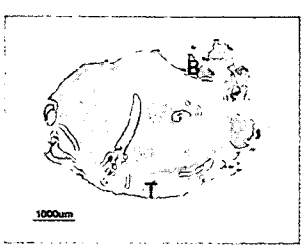


Fig. 6a

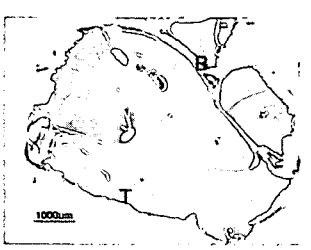


Fig. 6b

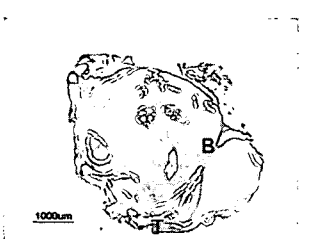


Fig. 6c

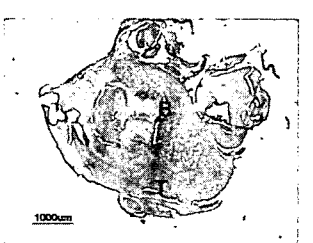


Fig. 6d

Histological findings at three weeks after the operation in a) the necrosis group, b) proximal suture group, c) partial tenotomy group and d) periosteal excision group. T, tendon stump; B, bone (all sections: magnification x 2; scale bar,1000 µm).

setting, Wakisaka et al[13] investigated the importance of the periosteum in a patient undergoing bone lengthening. Our results showed that callus formation occurred at sites where the periosteum was intact, but was deficient where it had been excised.

We demonstrated that a viable tendon stump, mechanical stress, and intact periosteum were all important for callus formation at the site of tendon reattachment. Further studies are necessary to clarify the role of callus in the integration of tendon and bone.

No benefits in any form have been received or will be received from a commercial party related directly or indirectly to the subject of this article.

## References

1. **Lee SK, Kubiak EN, Liporace FA, et al.** Fixation of tendon grafts for collateral ligament reconstructions: a cadaveric biomechanical study. *J Hand Surg [Am]* 2005;30:1051-5.
2. **Rufai A, Ralphs JR, Benjamin M.** Ultrastructure of fibrocartilages at the insertion of the rat Achilles tendon. *J Anat* 1996;189:185-91.
3. **Raspanti M, Strocchi R, De Pasquale V, et al.** Structure and ultrastructure of the bone/ligament junction. *Ital J Anat Embryol* 1996;101:97-105.
4. **Sano H, Kumagai J, Sawai T.** Experimental fascial autografting for the supraspinatus tendon defect: remodelling process of the grafted fascia and the insertion into bone. *J Shoulder Elbow Surg* 2002;11:166-73.
5. **Liu SH, Panossian V, al-Shaikh R, et al.** Morphology and matrix composition during early tendon to bone healing. *Clin Orthop* 1997;339:253-60.
6. **Leung KS, Qin L, Fu LK, et al.** A comparative study of bone repair and bone to tendon healing in patella: patella tendon complex in rabbits. *Clin Biomech (Bristol, Avon)* 2002;17:594-602.
7. **Rodeo SA, Arnoczky SP, Torzilla PA, et al.** Tendon-healing in a bone tunnel: a biomechanical and histological study in the dog. *J Bone Joint Surg [Am]* 1993;75-A:1795-803.
8. **Silva MJ, Ritty TM, Ditsios K, et al.** Tendon injury response: assessent of biomechanical properties, tissue morphology and viability following flexor digitorum profundus tendon transection. *J Orthop Res* 2004;22:990-7.
9. **Kessler I.** The "grasping" technique for tendon repair. *The Hand* 1973;5:253.
10. **Ohno K, Yasuda K, Yamamoto N, et al.** Effects of complete stress-shielding on the mechanical properties and histology of in situ frozen patellar tendon. *J Orthop Res* 1993;11:592-602.
11. **Stocum DL.** Frontier in medicine: regeneration. *Science* 1997;276:59-87.
12. **Kojimoto H, Yasui N, Goto T, et al.** Bone lengthening in rabbits by callus distraction: the role of periosteum and endosteum. *J Bone Joint Surg [Br]* 1988;70-B:543-9.
13. **Wakisaka T, Yasui N, Kojimoto H, et al.** A case of short metatarsal bones lengthened by callus distraction. *Acta Orthop Scand* 1988;59:194-6.

RESEARCH REPORT

# Study on factors related to loss of lower extremity muscle mass in elderly acute stroke patients

*Ayako Tamura*[1], *Takako Ichihara*[1], *Shinjiro Takata*[2], *Takako Minagawa*[1], *Yumi Kuwamura*[1], *Takae Bando*[1], *Natuo Yasui*[2], *and Shinji Nagahiro*[3]

[1]*Major in Nursing, School of Health Science, The University of Tokushima, Japan*

[2]*Department of Orthopedies, and* [3]*Department of Neurosurgery, Institute of Health Biosisciences, The University of Tokushima Graduate School, Tokushima, Japan*

**Abstract** The present study investigated the factors contributing to the loss of upper and lower extremity muscle mass in three elderly stroke patients with right hemiplegia in whom our rehabilitation program could not be performed at 1-2 weeks after onset. The results revealed common factors such as prolonged accurate microinjection of hypotensive agents, severe hemiplegia (Brunnstrom stage I or II), diarrhea and delayed initiation of tube feeding at 3 to 8 days after onset. With regard to individual differences, while all patients were recovering in bed, the degree of decrease in muscle mass varied among patients because they moved their extremities differently.

*Key words* : elderly, acute stroke patients, loss of lower extremity muscle mass, related factors

## Introduction

In recent years, the importance of rehabilitation during the acute phase of stroke is being recognized, and the notion that rehabilitation must begin during the acute phase is becoming more widely accepted. However, when providing nursing care to acute stroke patients, it is necessary to provide seemingly contradictory treatments, i.e., rest as part of acute patient management and exercise to prevent disuse syndrome. Hence, patients tend to remain rested in bed. Studies have been conducted using CT and DXA to analyze disuse muscle atrophy (reduced muscle mass) in cerebrovascular disorder patients[1-3]. Disuse muscle atrophy occurs on not only the paralyzed side, but also the unaffected side, and for prevention, studies have reaffirmed the necessity of placing patients in anti-gravity postures, such as sitting and standing positions, beginning in the acute phase[4-5]. However, in actual clinical settings, it is not possible to actively perform rehabilitation on elderly patients with cerebrovascular disorders due to complications such as fever and diarrhea.

Here, we examined three elderly stroke patients with right hemiplegia in whom our rehabilitation program could not be performed during the acute phase.

## Objective

The present study investigated and compared three elderly patients with right hemiplegia in whom our rehabilitation program could not be performed at 1-2 weeks after onset in order to identify the factors related to the loss of lower extremity muscle mass. The re-

2007年1月31日受付
2007年5月1日受理
別刷請求先：田村綾子，〒770-8509 徳島市蔵本町3-18-15
徳島大学医学部保健学科看護学専攻

sults of the present study should aid acute-phase recovery in elderly stroke patients.

## Terminology

The early phase of stroke was defined as within two weeks of onset.

## Methods

### 1. Subjects and Methods

Of stroke patients who were admitted on emergency to our hospital, subjects were those in whom a rehabilitation program designed by the authors could not be performed. In order to maintain consistency in disease conditions, three right-handed patients with right hemiplegia were selected.

The lower and upper extremity muscle mass of the three patients was measured by DXA (USA; Hologic Inc., QDR Delphi). The first measurement was performed at 3-5 days after onset, and the second measurement was performed at 7 days after the first measurement. Consciousness level, nutritional status, body weight and lower extremity circumference were measured twice at the same time as DXA. Other data were obtained from medical charts.

In the three patients, comparative analysis was conducted using the following 19 attributes and predictors for low lower extremity muscle : age, gender, disease, main therapy, accompanying disease, treatment, paralyzed side, affected-side motor function (Brunnstrom stage), consciousness level, swallowing disorder, aphasia, communication level, other relevant symptoms, nutritional status (TP : total protein), start of oral intake after admission, diet, length of infusion, activity level, body weight and lower extremity circumference.

The rehabilitation program that we designed was an exercise program that was separate from the rehabilitation programs designed by nurses and physical therapists. The rehabilitation program was not performed when patients did not meet the program criteria.

### 2. Ethical considerations

The present study was conducted after receiving the approval of the Ethics Committee for Clinical Research at Tokushima University Hospital. The contents of the study were explained to the subjects and their families. Upon verbal and written explanation that participation was voluntary, that nobody would be disadvantaged in medical treatment and nursing due to discontinuation or lack of participation in the study, and that privacy would be protected, agreement to participate was obtained in writing.

## Results

### 1. Decreased muscle mass

Table 1 shows the muscle mass and the degree of decrease in the upper and lower extremities on the paralyzed and unaffected sides, as assessed by DXA.

Table 1 Comparison of upper and lower extremity muscle mass among the three patients

| | Case A | Case B | Case C | Mean(SD) |
|---|---|---|---|---|
| Lower extremity muscle mass (DXA) | | | | |
| Paralyzed side, first test (g) | 4,831 | 6,307 | 5,664 | 5,600(661) |
| Paralyzed side, second test (g) | 4,568 | 5,752 | 5,073 | 5,131(502) |
| Difference (Second test-First test) (g) | −263 | −555 | −591 | −469(179) |
| Degree of decrease (%) | −5.4% | −8.8% | −10.4% | |
| Unaffected side, first test (g) | 4,743 | 6,060 | 4,958 | 5,253(706) |
| Unaffected side, second test (g) | 4,382 | 5,526 | 4,780 | 4,896(580) |
| Difference (Second test-First test) (g) | −361 | −534 | −174 | −357(178) |
| Degree of decrease (%) | −7.6% | −8.9% | −3.5% | |
| Upper extremity muscle mass (DXA) | | | | |
| Paralyzed side, first test (g) | 2,427 | 2,727 | 2,282 | 2,478(227) |
| Paralyzed side, second test (g) | 2,194 | 2,833 | 2,221 | 2,416(361) |
| Difference (Second test-First test) (g) | −274 | 106 | −61 | −62(169) |
| Degree of decrease (%) | −11.3% | +3.9% | −2.7% | |
| Unaffected side, first test (g) | 1,912 | 2,275 | 2,000 | |
| Unaffected side, second test (g) | 1,812 | 2,398 | 1,934 | 2,062(189) |
| Difference (Second test-First test) (g) | −100 | 123 | −66 | 2,051(305) |
| Degree of decrease (%) | −5.2% | +5.4% | −3.3% | −11(111) |

Degree of decrease = (Second-test muscle mass-First-test muscle mass)/First-test muscle mass × 100%